In Vivo Near-Infrared Fluorescence Imaging of Integrin $\alpha_2\beta_1$ in Prostate Cancer with Cell-Penetrating-Peptide–Conjugated DGEA Probe

Chiun-Wei Huang, Zibo Li, and Peter S. Conti

Molecular Imaging Center, Department of Radiology, University of Southern California, Los Angeles, California

The overexpression of integrin $\alpha_2\beta_1$ has been demonstrated to correlate with prostate tumor aggressiveness and metastatic potential. Recently, we reported that the DGEA peptide is a promising targeting ligand for near-infrared fluorescence and microPET imaging of integrin $\alpha_2\beta_1$ expression in prostate cancers. Here, we aimed to further improve the targeting efficacy of this peptide by incorporating a series of cell-penetrating peptides (CPPs) into the DGEA sequence. **Methods:** After the conjugation with appropriate fluorescent dyes, the CPP-DGEA peptides were evaluated in human prostate cell lines (PC-3, CWR-22, and LNCaP) that contain different integrin $\alpha_2\beta_1$ expression levels. In addition, to reduce excess kidney uptake, a carboxypeptidase-specific sequence Gly-Lys was incorporated into the probe design, allowing for cleavage by the kidney brush border enzymes of the CPP before uptake by proximal tubule cells. **Results:** Although the CPP motif greatly facilitated the translocation of CPP-DGEA without affecting binding specificity *in vitro*, fluorescent dye–labeled CPP-DGEA demonstrated extremely high kidney uptake *in vivo*. Kidney uptake was dramatically decreased after a carboxypeptidase-specific peptide linker (Gly-Lys) had been incorporated into the probe design. The optimized probe demonstrated a prominent accumulation of activity in PC-3 tumor (integrin $\alpha_2\beta_1$–positive). Receptor specificity was confirmed with blocking experiments and evaluation in a CWR-22 control tumor model with low $\alpha_2\beta_1$ expression. **Conclusion:** This study demonstrated that the introduction of a CPP sequence can facilitate the internalization of an integrin-targeted peptide probe *in vitro*. Moreover, a cleavable peptide linker successfully reduced kidney uptake while preserving good tumor uptake *in vivo*.

Key Words: prostate cancer; integrin $\alpha_2\beta_1$; cell penetrating peptides; prognostic marker

J Nucl Med 2011; 52:1979–1986
DOI: 10.2967/jnumed.111.091256

Malignant carcinoma of the prostate is the most frequently diagnosed noncutaneous malignancy and the second leading cause of cancer-related deaths among men in the United States (*1*). Although the prostate-specific-antigen screening test has greatly increased the number of patients identified with early-stage prostate cancer, who can be cured by radical prostatectomy, about 40% of prostate cancers are still first detected at an advanced stage, and half of these are found to be extracapsular at pathologic staging (*2–4*). Therefore, development of an accurate noninvasive imaging technique to detect primary, recurrent, and residual prostate cancer is critical for the effective management of this group of patients.

In hormone-refractory prostate cancers, $\alpha_2\beta_1$ integrin has been implicated in multiple aspects of tumor progression and metastasis (*5–12*). Because of the possible correlation between upregulation of integrin $\alpha_2\beta_1$ and tumor progression in human prostate cancer, noninvasive imaging of this receptor with radiolabeled peptides that specifically target integrin $\alpha_2\beta_1$ could therefore be useful to decipher the invasive potential of prostate cancers. Previously, we successfully developed various integrin $\alpha_2\beta_1$-targeted probes for prostate cancer imaging based on DGEA peptides, and promising results were obtained in both optical and PET imaging *in vivo* (*13–15*). However, these tracers cleared quickly through the renal pathway and the tumor washout rates were fast, as could be caused by the lack of a trapping mechanism. To enhance tumor uptake and retention, an attractive solution is to facilitate the internalization of DGEA peptides to integrin $\alpha_2\beta_1$-positive cells. Cell-penetrating peptides (CPPs) have been used to facilitate internalization and trapping of the labeled peptide probe at the target site. A common property shared among most CPPs is the abundance of arginine residues within their sequences, which are cationic and critical for membrane-translocating abilities (*16,17*). The ability of arginine-containing peptides to penetrate cells has been exploited by several groups. Simple arginine oligomers of varying lengths have been shown to effectively translocate across cell membranes of a variety of cell types (*16,18–22*). In this study, a series of CPP-conjugated DGEA peptides

Received Apr. 4, 2011; revision accepted Aug. 17, 2011.
For correspondence or reprints contact: Peter S. Conti, Department of Radiology, University of Southern California, 1510 San Pablo St., Room 350, Los Angeles, CA 90033.
E-mail: pconti@usc.edu
Published online Nov. 7, 2011.

was designed and evaluated for optical imaging of prostate cancer by targeting integrin $\alpha_2\beta_1$.

MATERIALS AND METHODS

General

All commercially available chemical reagents were used without further purification. 5(6)-Carboxyfluorescein, 9-fluorenylmethoxycarbonyl (Fmoc) amino acids, and Wang resin preloaded with the Fmoc-Ala amino acid were purchased from Novabiochem. Aspartic acid and glutamic acid were all protected as the tert-butyl ester. Cy5.5 monofunctional *N*-hydroxysuccinimide ester (Cy5.5-NHS) was purchased from Amersham Biosciences. The crude product was purified on an analytic reversed-phase high-performance liquid chromatography system equipped with a dual ultraviolet absorbance detector (model 2487; Waters) using a C18 reverse-phase (250 × 4.6 mm and 5 μm; Phenomenex) column. The flow was 1 mL/min, with the mobile phase starting from 98% solvent A (0.1% trifluoroacetic acid in water) and 2% solvent B (0.1% trifluoroacetic acid in acetonitrile) (0–2 min) and ending with 40% solvent A and 60% solvent B at 30 min.

Synthesis of Peptides

All peptides used in this study were chemically synthesized by Fmoc solid-phase peptide synthesis on Wang resin. Fmoc-Lys (Fmoc) was used as a building block for branching polyarginine peptide structures. Four equivalents of Fmoc–amino acid derivatives, benzotriazole-1-yl-oxy-tris-pyrrolidino-phosphoniumhexafluoro phosphate (PyBOP), and hydroxybenzotriazole, and an 8-fold molar excess of diisopropylethylamine (Sigma) per amino function, were used for each coupling. Acylation was performed for 60 min, and reaction completion was confirmed by the trinitrobenzene sulfonic acid test. The Fmoc protective group on the α- or ϵ-amino group was removed with 20% piperidine in dimethylformamide (v/v) (Sigma). Dimethylformamide was used to wash the resin between each acylation and deprotection step. Deprotection of the peptide and cleavage from the resin were conducted by treatment with a 95:5 mixture of trifluoroacetic acid:H_2O at room temperature for 3 h.

Fluorescent Dye Conjugation and Purification

FAM was coupled onto the exposed amino group at a 3-fold excess in the presence of equimolar amounts of PyBOP and a 6-fold molar excess of diisopropylethylamine for 2 h in the dark. The Cy5.5 conjugates were synthesized through conjugation of Cy5.5-NHS ester with the exposed amino group of the DGEA peptide probes. The Cy5.5-NHS, dissolved in dimethylformamide, was added to the fully protected DGEA peptide, which was still on the resin, followed by the addition of diisopropylethylamine (10-fold). The reaction mixture was stirred overnight in the dark at room temperature. After the conjugation, unbound FAM or Cy5.5 was removed by washing the resin with dimethylformamide, and the conjugated peptide DGEA was then cleaved from the resin by treating with cleavage solution (95% trifluoroacetic acid and 5% water) for 3 h. Crude peptides were precipitated and washed twice with ice-cold diethylether and dissolved in 10% acetic acid in water before lyophilization. The conjugated peptides were purified and characterized by analytic high-performance liquid chromatography, and fractions containing dye conjugates were collected, lyophilized, and stored in the dark at −20°C until used. The purity of labeled peptides was more than 95% from analytic high-performance liquid chromatography analysis. The identity of the products was ascertained using a LTQ Orbitrap Hybrid Mass Spectrometer (Thermo).

Cell Lines

The human prostate cancer cell line PC-3 was obtained from American Type Culture Collection and maintained at 37°C in a humidified atmosphere containing 5% CO_2 in F-12K medium and 10% fetal bovine serum (Life Technologies, Inc.). CWR-22 and LNCaP cell lines were also from American Type Culture Collection and grown in RPMI-1640 with 10% fetal bovine serum in 5% CO_2 at 37°C. The LNCaP and CWR-22 human prostate cancer cell lines express androgen receptors and prostate-specific antigens and are stimulated by dihydroxytestosterone. The PC-3 human prostate cancer cell line was initiated from a bone metastasis of a grade IV prostatic adenocarcinoma and displays low testosterone-5-α-reductase activity.

Flow Cytometry Study

Human prostate PC-3, CWR-22, and LNCaP cancer cells were used to assess cell binding and internalization efficiencies of $\alpha_2\beta_1$-targeted peptide probes. To minimize nonspecific uptake of peptides by pinocytosis, incubations were performed on ice followed by flow cytometric analysis to allow rapid quantification of fluorescence. To acquire the quantification of fluorescence by flow cytometry (FACScan; Becton Dickinson), 10,000 cells were counted and viable cells with similar size and granularity in the forward- and side-scatter plots were analyzed. The fluorescence profiles and the overall mean fluorescent intensities of the cells within this region were obtained and analyzed using CellQuest Software (Becton Dickinson).

In Vitro Fluorescence and Confocal Microscopy Studies

For fluorescence microscopy studies, PC-3, CWR-22, and LNCaP prostate cells (1×10^5) were cultured on Falcon 4 chamber vessel culture slides (BD Biosciences). After 24 h, the cells were washed twice with phosphate-buffered saline and then incubated at 25°C in the presence of an equimolar amount of fluorescent-dye–labeled peptide for 30 min. After the incubation period, the cells were washed 3 times with ice-cold phosphate-buffered saline. For the blocking study, an excess of unconjugated DGEA peptide was added to the binding medium before the addition of fluorescent-dye–labeled DGEA peptide conjugates. The fluorescence signals from the cells were recorded using an Axioskop 40 microscope (Carl Zeiss Micro-Imaging, Inc.) equipped with a fluorescein isothiocyanate filter set (exciter, 475/20 and 540/30 nm). An AttoArc HBO 100-W microscopic illuminator (Carl Zeiss Micro-Imaging, Inc.) was used as a light source for fluorescence excitation. Images were taken using a thermoelectrically cooled charged-coupled device (Micromax, model RTE/CCD-576; Princeton Instruments, Inc.).

PC-3 cells were further examined by confocal microscopy using a Bio-Rad 1024 MRC instrument (LS&E Infrastructure Unit). Green fluorescence was induced at a wavelength of 494 nm with a krypton and argon laser and detected at 550 nm. The photomultiplier gain and laser power levels were set by adjusting them such that the background fluorescence of cells incubated with phosphate-buffered saline was not visible.

Tumor Xenografts

Animal procedures were performed according to a protocol approved by the University of Southern California Institutional Animal Care and Use Committee. In the procedure, 4- to 6-wk-old 20- to 30-g noncastrated male athymic mice (BALB/c *nu/nu*) were injected subcutaneously with PC-3 and CWR-22 human prostate cancer cells (American Type Culture Collection) at a concentration of 1×10^6 cells per 0.1 mL in the shoulder, and enough time was allowed for tumors to grow to at least 3 mm in diameter (14–21 d after implantation). Tumor volume was calculated using the formula $S^2 \times L/2$, where S and L represent the small and large diameters, respectively, of the lesion. The mice were fed with Teklad Global 18% Protein Rodent Diet (Ralston Purina Co.) to reduce the autofluorescent signal for at least 11 d before they underwent any optical imaging, and they were maintained on a cycle of 12 h of light and 12 h of darkness.

In Vitro Near-Infrared Optical Imaging of Tumors

In vivo fluorescence imaging was performed with an IVIS 200 small-animal imaging system (Xenogen). A Cy5.5 filter set was used for acquiring the Cy5.5-conjugated DGEA peptide probe fluorescence *in vivo*. Identical illumination settings (lamp voltage, filters, f-stop, field of views, and binning) were used for acquiring all images, and fluorescence emission was normalized to photons/s/cm^2/steradian (sr). Images were acquired and analyzed using Living Image 4.0 software (Xenogen). For the control experiment, peptide probes were injected into 3 mice via the tail vein with 1.5 nmol of Cy5.5-conjugated DGEA peptide probes, and the animals underwent optical imaging at various time points after injection. For the blocking experiment, the mice ($n = 3$) for each probe were also injected with a mixture of 10 mg/kg of unlabeled DGEA peptide and 1.5 nmol of Cy5.5-conjugated DGEA peptide probes. All near-infrared fluorescence images were acquired using a 1-s exposure time (an f-stop of 4). The mice of the experimental and blocking groups were euthanized at 28 h after injection. The tumor and major tissues and organs were dissected, and ex vivo fluorescence images were obtained. To determine the localization and distribution of the probe, the tumor was dissected, placed in tissue holders, filled with Tissue-Tec optimal-cutting-temperature compound (Sakura Finetek USA, Inc.), and immediately frozen in dry ice. Fresh-tumor-tissue slides (5 μm) were obtained with a tissue slicer and imaged with fluorescence microscopy.

Data Processing and Statistics

All data are given as the mean ± SD of 3 independent measurements. Statistical analysis was performed with a Student *t* test. Statistical significance was assigned at the 95% confidence level, with a *P* value of less than 0.05.

RESULTS

In Vitro Characterization of CPPs-DGEA Peptide

FAM-DGEA, CPP-conjugated branched R4-FAM-DGEA peptide (Fig. 1), and nonsense peptide R4-FAM-AAAA were incubated with prostate cancer cell lines for flow cytometry analysis studies to evaluate the $\alpha_2\beta_1$ integrin binding specificity and affinity. The flow cytometry results demonstrated that the mean cell fluorescence intensities of PC-3 cells incubated with polyarginine peptide R4 FAM-DGEA were almost 2 times higher than the FAM-DGEA–incubated one, and the selectivity among different cell lines was maintained. The nonsense peptide R4-FAM-AAAA resulted in only minimal fluorescent signal (Supplemental Figs. 1A and 1B; supplemental materials are available online only at http://jnm.snmjournals.org). These observations clearly demonstrated that the CPP structure can enhance the binding affinity of DGEA peptide probes without compromising binding specificity among the tested prostate cancer cell lines.

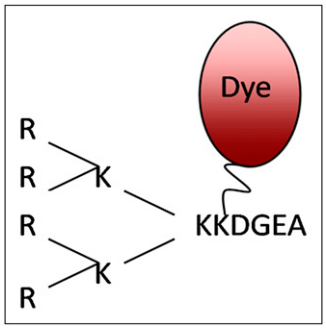

FIGURE 1. Peptide structure of R4-dye-DGEA. Peptide was labeled with FAM dye for *in vitro* study and Cy5.5 for *in vivo* imaging experiments.

The binding specificities and subcellular localizations of the R4-conjugated DGEA peptides were also examined using fluorescence microscopy, which showed that R4-FAM-DGEA bound distinctly to PC-3 cells whereas CWR-22 and LNCaP showed substantially lower levels of cellular fluorescent signals (Supplemental Fig. 1C). In addition, binding of the fluorescent DGEA probes could be blocked with the unlabeled DGEA peptide, doubly confirming that R4-FAM-DGEA peptide binding is $\alpha_2\beta_1$ integrin–specific. In these microscopy images, PC-3 cells incubated with R4-FAM-DGEA peptide unexpectedly seemed to show a strong signal from nuclear sites. Therefore, the intracellular localization of R4-FAM-DGEA was further examined by confocal microscopy. PC-3 cells that were incubated with R4-FAM-DGEA did exhibit a strong fluorescent signal inside the nucleus (Fig. 2). In comparison, the signals were confined mostly to the cytosol and cell membrane when FAM-DGEA peptides were used.

In Vitro Characterization of CPP-DGEA Peptides by Fluorescence Imaging

Receptor-specific uptake was evaluated *in vivo* using athymic nude mice bearing either the integrin $\alpha_2\beta_1$-positive PC-3 tumor or the control tumor CWR-22. Optical imaging was performed with an IVIS 200 small-animal imaging system (Xenogen). The whole animal became fluorescent immediately after injection, and the subcutaneous PC-3 tumor could clearly be delineated from the surrounding background tissue from 30 min to 24 h after injection. In addition, the CWR22 tumor demonstrated lower uptake than the PC-3 tumor for up to 4 h after injection, but the difference was not significant except at the first time point. In both tumor models, most of the injected fluorescent probes were trapped in the kidney (Supplemental Fig. 2). We believe this trapping could be caused by the rapid filtration of the probes

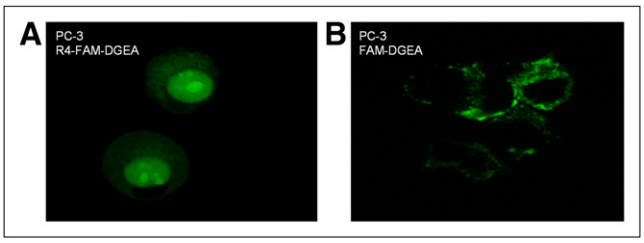

FIGURE 2. (A) Confocal imaging to further verify nucleus accumulation of R4-FAM-DGEA in PC-3 cells. (B) FAM-DGEA probe for comparison. Images showed that only R4-FAM-DGEA with CPP structure can predominantly accumulate inside nucleus of PC-3 cells.

and reabsorption by the kidney tubules in living mouse models.

CPP-DGEA Probes with Reduced Kidney Uptake

Previously, several possible approaches have been investigated to reduce kidney uptake. The use of organ-specific cleavable linkers was reported by Arano in 1998 (*23*). Based on that approach, we synthesized a DGEAGK targeting construct that comprised an N-terminal amino group and an ϵ-amino group (on C-terminal lysine) to regioselectively conjugate CPPs for cell penetration and a Cy5.5 dye for optical imaging. We anticipated that the peptide linker (Gly-Lys-OH) from the DGEA peptide probe could be cleaved by the kidney brush border enzymes before uptake by proximal tubule cells (because of the lysine-specific carboxypeptidase activity), thus reducing uptake of tracer by the kidney.

We first conjugated the Cy5.5 dye to the ϵ-amino group of C-terminal lysine without changing the original branched R4-DGEA peptide structure (Fig. 3A). The final probe, R4-DGEAGK(Cy5.5)-OH, was obtained at more than 95% purity with high-performance liquid chromatography, and the identity was confirmed by mass spectrometry (calculated, 2,482.88; observed, 2483.27). We assumed that the Cy5.5 dye could be released from the major peptide probe structure once the kidney carboxypeptidase recognized the Gly-Lys sequence. As shown in Figure 3A, the subcutaneous PC-3 tumor was clearly distinguished from the surrounding background tissue, and contrast was improved at late time points. Tumor uptake kept increasing with time and was almost equal to kidney uptake at 4 h after injection. The target-binding specificity was confirmed by the significantly decreased tumor uptake in the CWR22 model. Overall, uptake of R4-DGEAGK(Cy5.5)-OH by the kidney was dramatically decreased even though still slightly higher than the PC-3 tumor uptake. These results indicate that the Gly-Lys linker design is a feasible strategy to reduce uptake of CPP-DGEA conjugates by the kidney.

As an alternative approach, we switched the conjugation sites of R4 and Cy5.5, and we prepared the Cy5.5-DGEAGK(R4)-OH probe for *in vivo* imaging evaluation (Fig. 3B). Cy5.5-DGEAGK(R4)-OH was obtained at 95% purity, and the identity was confirmed by mass spectrometry (calculated, 2482.88; observed, 2,482.52). In this design, the CPP sequence would be cleaved from the imaging probe to reduce kidney uptake. As shown in Figure 3B, prominent tumor uptake was observed, and the fluorescent signals cleared rapidly from normal tissue. The highest uptake in tumor was at 1 h after injection, and the tumor washout rate was fairly rapid over time. Tumor uptake was significantly higher ($P < 0.05$) for PC-3 xenografts than for the CWR-22 model (control tumor model) at all time points examined. Unlike the R4-DGEAGK(Cy5.5)-OH probe, the Cy5.5-DGEAGK(R4)-OH probe showed maximum kidney uptake at 1 h after injection, and the absolute value was lower than the PC-3 tumor uptake. The difference became marginal at 4 h after injection. Although kidney uptake was successfully reduced in this design, tumor uptake and retention were also compromised, suggesting that further optimization is necessary.

In the imaging study of Cy5.5-DGEAGK(R4)-OH, we believe the observed fast probe clearance could be attributed to the steric hindrance of the R4 branch structure, which may interfere with binding of DGEA and integrin $\alpha_2\beta_1$. To verify this hypothesis, we introduced a linear R8 CPP structure into the probe design (Supplemental Fig. 3). The Cy5.5-DGEAGK(R8)-OH peptide probe was obtained at 95% purity, and the identity was confirmed by mass spectrometry (calculated, 2,723.11; observed, 2,723.48).

The *in vivo* distributions of Cy5.5-DGEAGK(R8)-OH in PC-3 and CWR-22 tumor-bearing mice are shown in Figure 4. PC-3 tumor was clearly visualized at the early time, with a good tumor-to-kidney ratio. In addition to showing reduced kidney uptake, the CWR-22 tumor demonstrated much lower peptide uptake than the PC-3 tumor ($P < 0.05$), thus demonstrating the receptor specificity of the Cy5.5-DGEAGK(R8)-OH probe. To further validate the targeting specificity of the Cy5.5-DGEAGK(R8)-OH peptide probe, we performed a blocking experiment (Supplemental Fig. 4). The same amount of Cy5.5-DGEAGK(R8)-OH probe was coinjected with a 10 mg/kg dose of unlabeled DGEA peptide (300 nmol), and imaging was performed at 2 h after injection. PC-3 tumor uptake was successfully reduced by the unlabeled DGEA peptide, confirming the receptor specificity of this probe. Immunofluorescent staining of both tumor tissues with the monoclonal antibody fluorescein isothiocyanate antihuman CD49b (BioLegend) was also performed to validate the expression level of integrin $\alpha_2\beta_1$ (Supplemental Fig. 5).

After promising imaging results were obtained, we further investigated whether Cy5.5-DGEAGK(R8)-OH can translocate into tumor cells after specific binding with integrin $\alpha_2\beta_1$ *in vivo*. To answer this question, we studied the spatial distribution of Cy5.5-DGEAGK(R8)-OH by performing fluorescence microscopy imaging of fresh tissue slides (Supplemental Fig. 6). Cy5.5-DGEAGK(R8)-OH peptide indeed accumulated inside the tumor cells, in addition to outside the vascular space in stroma and tumor cells

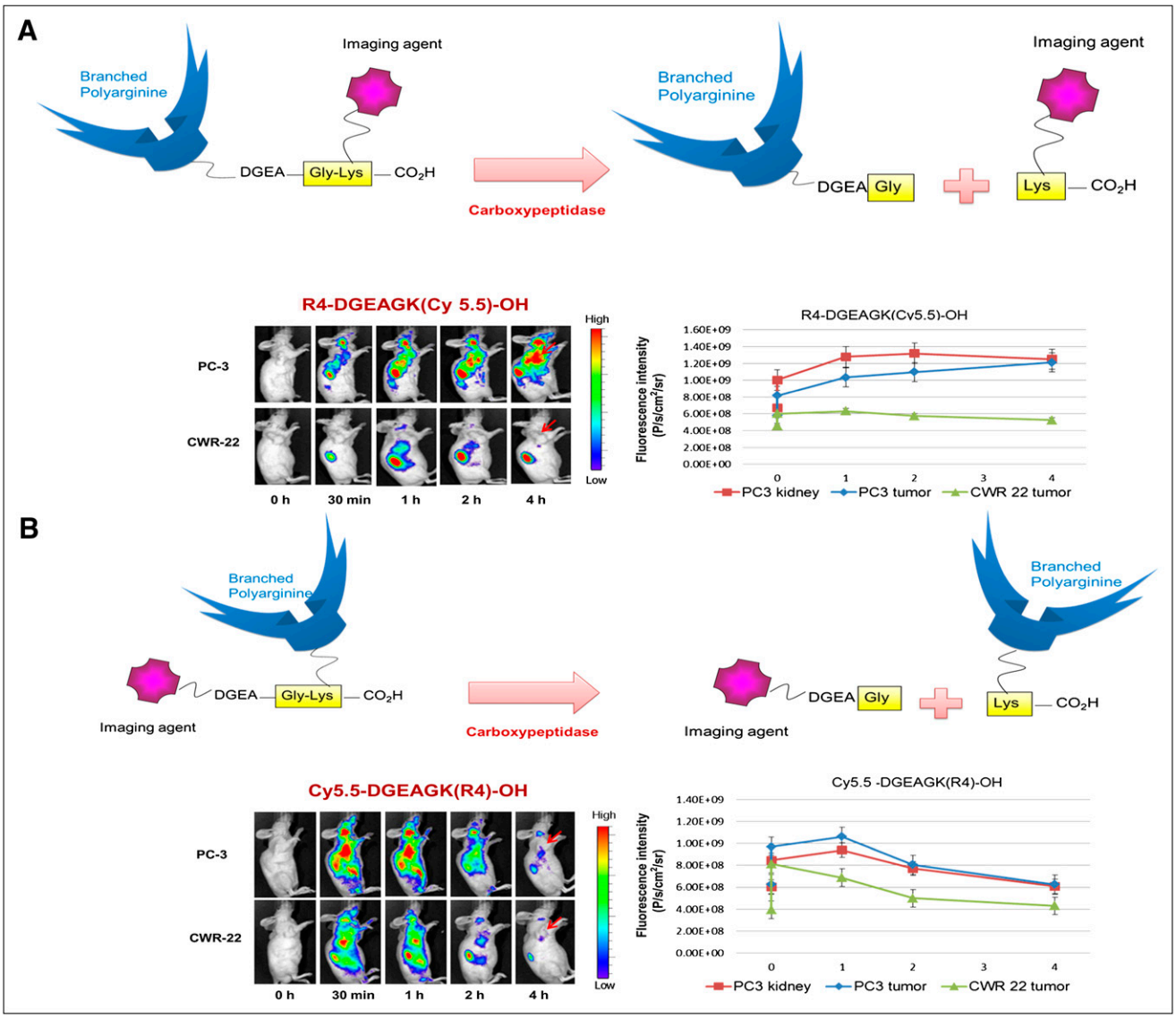

FIGURE 3. Schematic structure of cleavable CPP-DGEA probe design that consisted of brush border peptidase–sensitive linker (Gly-Lys-OH), DGEA-targeting sequence, and Cy5.5 and CPPs. *In vivo* fluorescence imaging and quantification plots are shown for athymic nude mice bearing subcutaneous PC-3 or CWR-22 xenografts (n = 3 for each model) after intravenous injection of 1.5 nmol of R4-DGEAGK (Cy5.5)-OH (A) or Cy5.5-DGEAGK(R4)-OH (B). Specificity of peptide uptake between 2 tumor models is not compromised. PC-3 tumor displayed higher peptide uptake and better tumor-to-normal contrast than that of CWR-22 tumor for both peptide probes. Kidney accumulation dropped dramatically after introduction of enzyme-specific linker.

(4,6-diamino-2-phenylindole was used for nuclear staining and is shown in blue in the figure).

DISCUSSION

Progression of prostate cancer primarily involves the formation of secondary metastatic lesions to bone. The role of integrin $\alpha_2\beta_1$ in tumor invasion and metastasis has been implicated by its increased expression in more aggressive prostate cancer. Previously, we reported the synthesis and biologic evaluation of a series of near-infrared fluorescent optical probes and PET tracers for integrin $\alpha_2\beta_1$-targeted imaging based on DGEA peptides. The DGEA-based peptide was concluded to be a promising ligand for integrin $\alpha_2\beta_1$ imaging *in vivo*. However, the fast washout rate from the tumor may somewhat limit application. We hypothesized that tumor retention might be greatly increased by introducing a selective trapping mechanism.

CPP-mediated bio-cargo delivery into living cells has attracted great attention in the last few decades (*24–26*). This novel technology has demonstrated great potential both for basic research in cellular biology and for therapeutic application. By hybridization of these CPPs genetically or chemically, efficient intracellular delivery of various oligopeptides and proteins has been achieved *in vitro* (*27–31*). Inspired by these results, we proposed that the CPP-conjugated

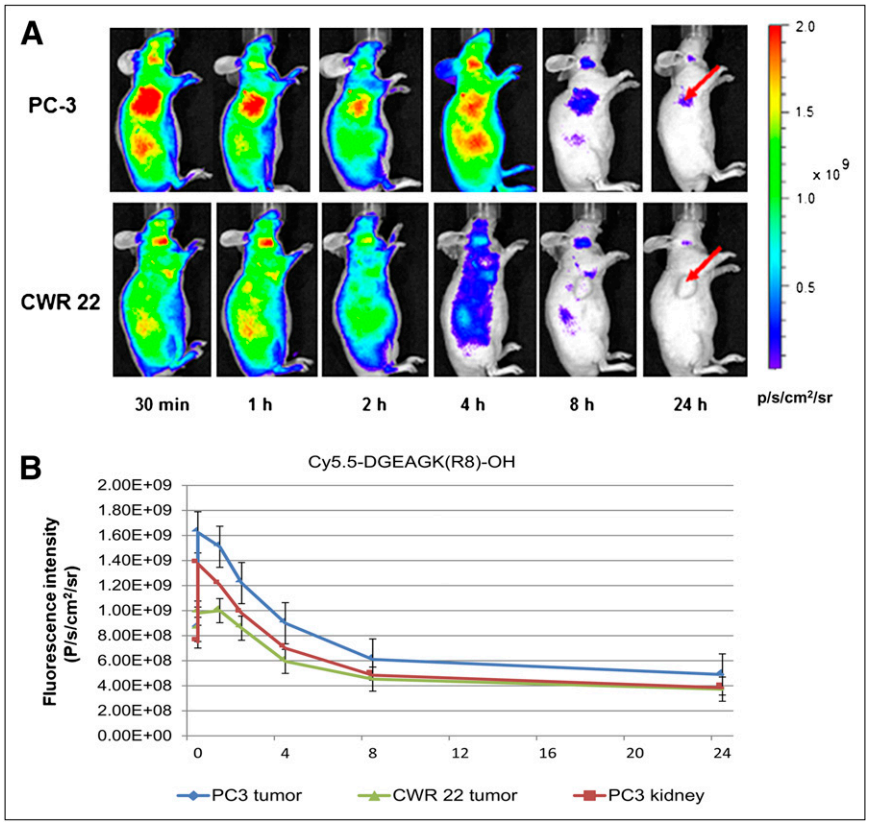

FIGURE 4. (A) *In vivo* fluorescence imaging of athymic nude mice bearing subcutaneous PC-3 or CWR-22 xenografts ($n = 3$ for each model) after intravenous injection of 1.5 nmol of Cy5.5-DGEAGK(R8)-OH. (B) Positive and control tumor models indicate that specificity of peptide probe was not compromised. PC-3 tumor showed higher probe uptake than that of CWR-22 tumor, and kidney uptake decreased dramatically because of cleavable linker. Compared with branch R4, linear R8 conjugate demonstrated improved tumor retention.

DGEA peptides may be able to cross cell membranes and be trapped inside the cell. This potential would greatly expand options for the design of our integrin $\alpha_2\beta_1$-targeted imaging agent.

In our initial approach, we conjugated the CPP and Cy5.5 dye to the distant N-terminal and ϵ-amino group of Lys and obtained the branched R4-K(Cy5.5)-DGEA peptide as a prototype probe. The branched polyarginine R4 structure was tested first because the branched structure may lead to a higher translocation ability, whereas linear counterparts with the same amount of arginine do not show significant internalization. Flow cytometry experiments demonstrated that the introduction of the additional R4 unit effectively enhanced cell-labeling efficiency without affecting binding specificity. Moreover, confocal imaging of the PC-3 cell also demonstrated the significantly increased cell retention of R4-FAM-DGEA, compared with FAM-DGEA. In fact, it was previously shown that integrin-targeted probes, such as cyanine dye–labeled cyclic RGD peptides, could be internalized to only a limited extent (*32*) and that the internalization is most likely attributable to the increased lipophilicity of the tagging of fluorescent dye (*33*). Clearly, the increased uptake for R4-FAM-DGEA should be caused mainly by incorporation of the CPP motif. The cell-penetrating property of this CPP-conjugated peptide probe not only improves integrin $\alpha_2\beta_1$-targeted binding but also provides a potential opportunity for therapy application. However, whether the nuclear penetration was related to $\alpha_2\beta_1$ integrin targeting is not fully understood. Further biologic investigations are required to elucidate the mechanism.

Despite the improved *in vitro* behavior of R4-K(dye)-DGEA, it demonstrated a prominent and persistent kidney uptake *in vivo*. Previous studies have demonstrated that the high kidney uptake of some imaging agents is related to the overall positive charge of the probes (*34–36*). Because we did observe much lower kidney uptake of our previously reported Cy5.5-DGEA probe, the prolonged kidney uptake of CPP-modified DGEA might be attributed to the positive charge on the CPP motif. Although it is a common phenomenon for peptide probes to have relatively high kidney uptake, potential clinical therapeutic applications might be limited for agents such as R4-DGEA, since the kidney usually is the dose-limiting organ. Therefore, a CPP-conjugated DGEA probe with improved *in vivo* pharmacokinetic behavior is needed to create an effective integrin $\alpha_2\beta_1$-targeted carrier for both diagnosis and therapy applications.

Previously, Arano reported that the Gly-Lys linker could be specifically cleaved by the brush border carboxypeptidase in the kidney (*23*). Here, we adopted this peptide linker strategy (Gly-Lys) in our integrin $\alpha_2\beta_1$-targeted probe design. R4-DGEAGK(Cy5.5)-OH, Cy5.5-DGEAGK(R4)-OH, and Cy5.5-DGEAGK(R8)-OH were prepared and evaluated in PC-3 and CWR22 tumor models. Kidney uptake was dramatically decreased in these CPP-DGEA peptides modified with the G-K linker. Tumor-targeting specificity was not affected in the tested prostate cancer models. These

imaging results demonstrated that the use of a cleavable peptide linker between the fluorescent dye–labeled DGEA tracer and polyarginine motif (CPP) is a feasible approach to lower kidney uptake while preserving tumor contrast. Among all the CPP-conjugated peptides, Cy5.5-DGEAGGK (R8)-OH is the most promising imaging agent because it has the highest tumor uptake and lowest kidney uptake. Currently, we are developing a radiolabeled tracer based on this construct. In summary, we have successfully developed CPP-DGEA–based optical agents for near-infrared fluorescence imaging of integrin $\alpha_2\beta_1$ expression in prostate cancer. We also demonstrated that kidney uptake of these newly designed probes could be effectively reduced after introduction of an organ-specific linker. The incorporation of additional strategies, such as the administration of L- or D-lysine, may further lower kidney uptake. Moreover, in view of the favorable trapping phenomena we have observed in this research, these integrin $\alpha_2\beta_1$-specific peptide probes not only may be used as diagnostic imaging agents but also may serve as an efficient drug delivery carrier for prostate cancer therapy.

CONCLUSION

Our results clearly demonstrated the great potential of using a CPP motif to enhance the tumor targeting and internalization capabilities of DGEA peptides. Moreover, it was shown that a cleavable peptide linker could successfully reduce kidney uptake while preserving good tumor uptake *in vivo*. The success of this research could lead to a selective and highly effective diagnostic imaging agent to evaluate the stage of prostate cancer, help us more appropriately select patients considered for potential antiintegrin $\alpha_2\beta_1$-based treatment, and allow the evaluation of disease course and therapeutic efficacy at the earliest stages of treatment. In view of their favorable trapping phenomena, the integrin $\alpha_2\beta_1$-specific peptides developed in this study may also serve as an efficient drug delivery carrier for prostate cancer therapy.

DISCLOSURE STATEMENT

The costs of publication of this article were defrayed in part by the payment of page charges. Therefore, and solely to indicate this fact, this article is hereby marked "advertisement" in accordance with 18 USC section 1734.

ACKNOWLEDGMENTS

This study was supported in part by the Molecular Imaging Center at USC, the James H. Zumberge Faculty Research and Innovation Fund, the National Cancer Institute (P30CA014089), ACS/IRG pilot project funds IRG-58-007-48, and research grant DE-SC0002353 from the Department of Energy. No other potential conflict of interest relevant to this article was reported.

REFERENCES

1. The Surveillance, Epidemiology, and End Results Program: cancer of the prostate statistics 2010. National Cancer Institute Web site. Available at: http://seer.cancer.gov/statfacts/html/prost.html. Accessed October 19, 2011.
2. Pashayan N, Pharoah P, Neal DE, et al. Stage shift in PSA detected prostate cancers: effect modification by Gleason score. *J Med Screen.* 2009;16:98–101.
3. Oesterling JE. Prostate specific antigen: a critical assessment of the most useful tumor marker for adenocarcinoma of the prostate. *J Urol.* 1991;145:907–923.
4. Potosky AL, Miller BA, Albertsen PC, Kramer BS. The role of increasing detection in the rising incidence of prostate cancer. *JAMA.* 1995;273:548–552.
5. Lochter A, Navre M, Werb Z, Bissell MJ. alpha1 and alpha2 integrins mediate invasive activity of mouse mammary carcinoma cells through regulation of stromelysin-1 expression. *Mol Biol Cell.* 1999;10:271–282.
6. Kirkland SC, Ying H. Alpha2beta1 integrin regulates lineage commitment in multipotent human colorectal cancer cells. *J Biol Chem.* 2008;283:27612–27619.
7. Patrawala L, Calhoun-Davis T, Schneider-Broussard R, Tang DG. Hierarchical organization of prostate cancer cells in xenograft tumors: the CD44+α2β1+ cell population is enriched in tumor-initiating cells. *Cancer Res.* 2007;67:6796–6805.
8. Kostenuik PJ, Sanchez-Sweatman O, Orr FW, Singh G. Bone cell matrix promotes the adhesion of human prostatic carcinoma cells via the alpha 2 beta 1 integrin. *Clin Exp Metastasis.* 1996;14:19–26.
9. Slack-Davis JK, Parsons JT. Emerging views of integrin signaling: implications for prostate cancer. *J Cell Biochem.* 2004;91:41–46.
10. Chung LWK, Baseman A, Assikis V, Zhau HE. Molecular insights into prostate cancer progression: the missing link of tumor microenvironment. *J Urol.* 2005;173:10–20.
11. Hall CL, Dai J, van Golen KL, Keller ET, Long MW, Type I collagen receptor (α2β1) signaling promotes the growth of human prostate cancer cells within the bone. *Cancer Res.* 2006;66:8648–8654.
12. Kiefer JA, Farach-Carson MC. Type I collagen-mediated proliferation of PC3 prostate carcinoma cell line: implications for enhanced growth in the bone microenvironment. *Matrix Biol.* 2001;20:429–437.
13. Huang CW, Li Z, Cai H, Shahinian T, Conti PS. Biological stability evaluation of the α2β1 receptor imaging agents: diamsar and DOTA conjugated DGEA peptide. *Bioconjug Chem.* 2011;22:256–263.
14. Huang C, Li Z, Cai H, Chen K, Shahinian T, Conti PS. Design, synthesis and validation of integrin α2β1-targeted probe for microPET imaging of prostate cancer. *Eur J Nucl Med Mol Imaging.* 2011;38:1313–1321.
15. Huang CW, Li Z, Cai H, Shahinian T, Conti PS. Novel $\alpha_2\beta_1$ integrin-targeted peptide probes for prostate cancer imaging. *Mol Imaging.* 2011;10:284–294.
16. Rothbard JB, Kreider E, VanDeusen CL, Wright L, Wylie BL, Wender PA. Arginine-rich molecular transporters for drug delivery: role of backbone spacing in cellular uptake. *J Med Chem.* 2002;45:3612–3618.
17. Sakai N, Matile S. Anion-mediated transfer of polyarginine across liquid and bilayer membranes. *J Am Chem Soc.* 2003;125:14348–14356.
18. Futaki S, Suzuki T, Ohashi W, et al. Arginine-rich peptides: an abundant source of membrane-permeable peptides having potential as carriers for intracellular protein delivery. *J Biol Chem.* 2001;276:5836–5840.
19. Futaki S. Arginine-rich peptides: potential for intracellular delivery of macromolecules and the mystery of the translocation mechanisms. *Int J Pharm.* 2002;245:1–7.
20. Futaki S. Membrane-permeable arginine-rich peptides and the translocation mechanisms. *Adv Drug Deliv Rev.* 2005;57:547–558.
21. Takayama K, Suehisa Y, Fujita T, et al. Oligoarginine-based prodrugs with self-cleavable spacers for caco-2 cell permeation. *Chem Pharm Bull (Tokyo).* 2008;56:1515–1520.
22. Futaki S, Goto S, Suzuki T, Nakase I, Sugiura Y. Structural variety of membrane permeable peptides. *Curr Protein Pept Sci.* 2003;4:87–96.
23. Arano Y. Strategies to reduce renal radioactivity levels of antibody fragments. *Q J Nucl Med.* 1998;42:262–270.
24. Vives E. Present and future of cell-penetrating peptide mediated delivery systems: "Is the Trojan horse too wild to go only to Troy? *J Control Release.* 2005;109:77–85.
25. Foerg C, Merkle HP. On the biomedical promise of cell penetrating peptides: limits versus prospects. *J Pharm Sci.* 2008;97:144–162.
26. Mäe M, Langel Ü. Cell-penetrating peptides as vectors for peptide, protein and oligonucleotide delivery. *Curr Opin Pharmacol.* 2006;6:509–514.
27. Vivès E, Brodin P, Lebleu B. A truncated HIV-1 Tat protein basic domain rapidly translocates through the plasma membrane and accumulates in the cell nucleus. *J Biol Chem.* 1997;272:16010–16017.
28. Fawell S, Seery J, Daikh Y, et al. Tat-mediated delivery of heterologous proteins into cells. *Proc Natl Acad Sci USA.* 1994;91:664–668.

29. Derossi D, Joliot AH, Chassaing G, Prochiantz A. The third helix of the Antennapedia homeodomain translocates through biological membranes. *J Biol Chem.* 1994;269:10444–10450.
30. Mitchell DJ, Kim DT, Steinman L, Fathman CG, Rothbard JB. Polyarginine enters cells more efficiently than other polycationic homopolymers. *J Pept Res.* 2000;56:318–325.
31. Nagahara H, Vocero-Akbani AM, Snyder EL, et al. Transduction of full-length TAT fusion proteins into mammalian cells: TAT-p27Kip1 induces cell migration. *Nat Med.* 1998;4:1449–1452.
32. Sancey L, Garanger E, Foillard S, et al. Clustering and internalization of integrin αvβ3 with a tetrameric RGD-synthetic peptide. *Mol Ther.* 2009;17:837–843.
33. Baker M, Ntam C, Reese CT, et al. Internalization of near-infrared fluorescent dyes within isolated leukocyte populations. *Int J Environ Res Public Health.* 2006;3:31–37.
34. Akizawa H, Uehara T, Arano Y. Renal uptake and metabolism of radiopharmaceuticals derived from peptides and proteins. *Adv Drug Deliv Rev.* 2008;60:1319–1328.
35. Behr TM, Sharkey RM, Juweid ME, et al. Reduction of the renal uptake of radiolabeled monoclonal antibody fragments by cationic amino acids and their derivatives. *Cancer Res.* 1995;55:3825–3834.
36. Boswell CA, Tesar DB, Mukhyala K, Theil F, Fielder PJ, Khawli LA. Effects of charge on antibody tissue distribution and pharmacokinetics. *Bioconjug Chem.* 2010;21:2153–2163.